RGD peptide immobilized on TiO$_2$ nanotubes for increased bone marrow stromal cells adhesion and osteogenic gene expression

Xin Cao · Wei-qiang Yu · Jing Qiu ·
Yan-fang Zhao · Yi-lin Zhang · Fu-qiang Zhang

Abstract Recently, TiO$_2$ nanotube layers are widely used in orthopedics and dental applications because of their good promotion effect on bone cells. Furthermore, peptide sequences such as arginine–glycine–aspartic acid are used to modify Ti implant for binding to cell surface integrins through motif. In this study, a cellular adhesive peptide of arginine–glycine–aspartic acid–cysteine (RGDC) was immobilized onto anodized TiO$_2$ nanotubes on Ti to examine its in vitro responses on rat bone marrow stromal cells (BMSCs). Materials were characterized by scanning electron microscopy (SEM) and X-ray photoelectron spectroscopy techniques. High-resolution C1s scans suggested the presence of RGDC on the surface and SEM images confirmed the nanotubes were not destroyed after modification. BMSCs adhesion and osteogenic gene expression were detected in TiO$_2$ nanotube layers with and without RGDC modification by fluorescence microscopy, confocal laser scanning microscopy, SEM, and realtime polymerase chain reaction (Real-time PCR). Results showed that the TiO$_2$ nanotube layers immobilized with RGDC increased BMSCs adhesion compared to nonfunctionalized nanotubes after 4 h of cultivation. Furthermore, the osteogenic gene expression of BMSCs was dramatically enhanced on the TiO$_2$ nanotube layers immobilized with RGDC (10 mM) compared to the TiO$_2$ nanotube layers immobilized with RGDC (1 mM) and non-functionalized anodized Ti.

Our results from in vitro study provided evidence that Ti anodized to possess nanotubes and then further functionalized with RGDC should be further studied for the design of better biomedical implant surfaces.

1 Introduction

It is well known that titanium (Ti) is a biocompatible orthopedic and dental material. Many methods have been developed to enhance the osseointegration of Ti-implant, such as increasing the surface roughness or altering the crystal structure and chemical composition [1–3]. Recently, the researchers started to simulate the topography of normal bone including collagen (mostly type I collagen 300 nm in length and 1.5 nm in diameter [4]) and hard inorganic nanocrystalline hydroxyapatite on implant surfaces [4]. Furthermore, the Ti implants with nanoscale structures have been confirmed as an efficacious method to enhance osteoblast function in vitro and osseointegration in vivo [5, 6].

Many researches on nano implant have been focused on TiO$_2$ nanotube layers by anodization through precisely controlling pore size and promoting bone formation [5–8] Oh et al. [5] firstly reported that the growth of osteoblast was increased by as much as $300 \sim 400\%$ on TiO$_2$ nanotube layers compared with unanodized titanium. The in vitro function of osteoblasts [5] and in vivo bone growth [6] were better on Ti implant with nanotubes than on conventional micro-roughened Ti surfaces. Furthermore, human mesenchymal stem cells (hMSCs) could preferentially differentiate into osteoblast-like cells on the TiO$_2$ nanotube surface without osteogenic inducing media [7]. Recently, we have studied the adhesion, proliferation, and differentiation of primary osteoblasts cultured in vitro on

X. Cao · W. Yu · J. Qiu · Y. Zhao · Y. Zhang · F. Zhang (✉)
Department of Prosthodontics, School of Stomatology
and Affiliated Ninth People's Hospital, School of Medicine,
Shanghai Research Institute of Stomatology, Shanghai Jiao Tong
University, Shanghai 200011, China
e-mail: fredzc@online.sh.cn; xuenaiangel1@sina.com

nanotube layers with different diameters [8]. Our results showed that preosteoblast cultured on 70 nm diameter nanotubes had relatively better adhesion and differentiation potential at the same time.

Extracellular matrix proteins are very important for controlling cell functions, including adhesion, proliferation, and differentiation [9]. Researches on the cell-attachment activities of various proteins, such as vitronectin, fibronectin, fibrinogen, and collagen, have revealed that oligopeptide sequences, including Arg–Gly–Asp (RGD), may act as ligands binding to the cell attachment receptor (integrin super family) on cell membranes [10]. Integrins are heterodimers formed by noncovalent association of α and β subunits that bind to a RGD motif, which is a peptide sequence present in many ECM proteins [11]. In the past few years, researchers argued that covalently immobilized RGD could promote cell attachment on various substrates [12, 13]. Bone formation was also accelerated by immobilizing RGD on a Ti surface [14]. Recently, Secchi [15] et al. found that RGDS peptides immobilized on titanium alloy stimulated bone cell differentiation. Therefore, immobilizing RGD peptides on materials have become an important strategy for designing implant surface. However, whether the RGD peptides have a significant influence on behavior of bone cells on implant surface with nanoscale features, which are effective approach to improve implants, is not exactly understood.

So in this study, it was hypothesized that the TiO_2 nanotubes by anodic oxidation have an effective influence on BMSCs adhesion and osteogenic gene expression after RGDC functionalization.

2 Materials and methods

2.1 TiO_2 nanotubes fabrication

The sample materials were commercial Ti thin foils (0.25 mm thick) with a purity of 99.5% (Alfa Aesar). First titanium substrates were immersed in a mixture (2 ml 48% HF, 3 ml 70% HNO_3 (both reagent grade chemicals) and 100 ml deionized water) for 5 min to remove the naturally formed oxide layer, then rinsing in deionized water and drying in nitrogen stream. The specimens were prepared by anodic oxidation process as reported previously [16]. The electrolyte for anodizing consisted of 1 M H_3PO_4 and 0.5 wt% HF. To obtain 70 nm diameter nanotubes on the anodized titanium surfaces, 15 V was used during the experiments in the electrolyte for 3 h. Platinum was used as the counter electrode. All anodic oxidation processes were carried out at room temperature. The samples were rinsed with deionized water and dried in a nitrogen stream after anodization.

2.2 Immobilization of RGDC peptide on TiO_2 nanotubes

An aminosilane linker was used to achieve RGDC peptide immobilization on TiO_2 nanotubes [17–19]. Silanization was carried out by immersing the substrates in 5% solution of (3-aminopropyl)-triethoxysilane (APTES) (Aldrich) in anhydrous hexane for 2 h (while stirring). After the reaction, the samples were washed twice with anhydrous hexane and ethanol and several times with deionized water. Then silanized substrates were incubated for 1 h at room temperature with a solution of 3.3 ml of N,N-dimethyl-formamide (DMF) (Sigma) containing 25 mg of N-succinimidyl-3-maleimidoproprionate (Aldrich). The maleimide-grafted membranes were then washed twice with DMF and several times with deionized water. To prevent hydrolysis, the membranes were immediately subjected to the next step and were incubated for 2 h at room temperature with 300 ml of pure water containing 1.35 mg or 0.135 mg of RGDC (Shanghai Bootech BioScience &Technology Co) for a final concentration of 10 mM and 1 mM. The RGDC-grafted membranes were thoroughly washed with deionized water, dried and stored at 4°C till further analysis.

2.3 Surface characterization

2.3.1 Scanning electron microscopy (SEM)

The surface morphology of the TiO_2 nanotubes and the immobilized RGDC on surfaces of TiO_2 nanotubes were examined by SEM using a microscope equipped with an energy-dispersive X-ray spectrometer (Philips, Netherlands, Sirion200).

2.3.2 X-ray photoelectron spectroscopy (XPS)

Surface chemistry after each stage of the modification protocol was assessed using XPS (VG Scientific Microlab 310F, East Grinstead, UK). The analysis was performed utilizing a monochromatic Al Ka electrode at 15 kV and 150 W at a 45 take-off angle. The sampling depth was measured about 3 nm. The Service Physics ESCAVB Graphics Viewer (Bristol, UK) program was used to determine peak areas.

2.4 Biological activity

2.4.1 Cell culture

Male Wistar rats of 4 week old with average weight of 100 g $\pm$ 15 g were obtained from the Ninth People's Hospital Animal Center (Shanghai, China). The study was

approval by the Institutional Animal Care and Use Committee of the Ninth People's Hospital Animal Center. Briefly, both ends of the femora were cut off at the epiphysis and the marrow was flushed out using Dulbecco's modified Eagle's medium (DMEM) (Gibco BRL, Grand Island, NY, USA) with 10% FBS (Hyclone, Logan, UT, USA) supplemented with 200 U/ml of heparin (Sigma, St. Louis, MO, USA). Rat bone marrow stromal cells (BMSCs) were cultured in DMEM with 10% fetal bovine serum and 1% penicillin/streptomycin (PS) under 37°C, 5% CO_2 environment. The medium was changed 24 h after inoculation to remove any unattached cells, and the remaining attached cells were considered as mainly BMSCs. Then media were changed three times every week until confluence was achieved. Cell osteogenic gene expression was detected after BMSCs were cultivated in osteogenic media (regular media described above plus 10 mM β-glycerol phosphate and 50 μM ascorbic acid (Sigma, Shanghai, China)). The BMSCs were seeded on a 24-well polystyrene plate (Falcon, USA) at a concentration of 3×10^4 cells/well. The specimens used in this research were randomly divided into four groups: (a) untreated TiO_2 nanotube layers, (b) APTES-silanized TiO_2 nanotube layers, (c) 1 mM RGDC-TiO_2 nanotube layers, and (d) 10 mM RGDC-TiO_2 Nanotube layers. Culture media were changed every 2 or 3 days. BMSCs of passages 2~4 were used for further experiment.

2.4.2 Cell morphology

After 4 and 24 h of cultivation, each disk was gently rinsed twice with PBS and then soaked in 0.1 M PBS with 2.5%

Table 1 Primer sequences

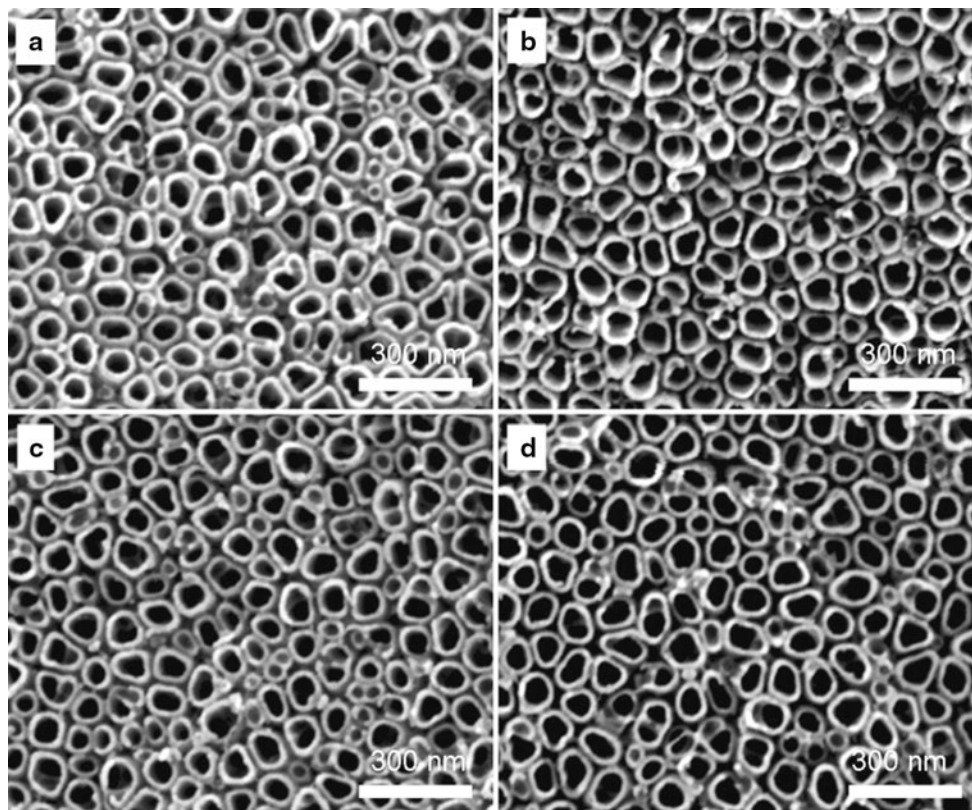| Gene	Sense primer (5′ to 3′)	Antisense primer (5′ to 3′)
RUNX2	ATCCAGCCACCTTCACTTACACC	GGGACCATTGGGAACTGATAGG
BMP-2	TGGGTTTGTGGTGGAAGTGGC	TGGATGTCCTTTACCGTCGTG
BSP	AGAAAGAGCAGCACGGTTGAGT	GACCCTCGTAGCCTTCATAGCC
OPN	CCAAGCGTGGAAACACACAGCC	GGCTTTGGAACTCGCCTGACTG
β-actin	CACCCGCGAGTACAACCTTC	CCCATACCCACCATCACACC

Fig. 1 SEM images of nanotube layers. **a** untreated TiO_2 nanotube layer. **b** APTES-silanized TiO_2 nanotube layers. **c** 1 mM RGDC-TiO_2 nanotube layers. **d** 10 mM RGDC-TiO_2 nanotube layers

glutaraldehyde for 1 h. After fixation, they were rinsed three times with PBS for 10 min. The disks were dehydrated in a graded series of alcohol (35, 50, 75, 90, and 100%) for 10 min and subsequently dried by supercritical point CO_2. SEM imaging was conducted on the field emission SEM after the surfaces were sputter coated in gold.

2.4.3 Cell adhesion

BMSCs were seeded on the substrates at a density of 3×10^4 cells/well on the titanium samples. After cell attachment for 4 h, a combination dye (Live/Dead Viability Assay Kit, ScienCell) was applied to assess the cell viability which can be displayed under fluorescence microscope. Due to changes in membrane integrity, living cells appear fluorescent green and dead cells appear fluorescent red. After 4 h culture on titanium dishes, cells were washed with PBS, and then added with working solution (Thaw and dilute appropriate volume of Live/Dead Cell Staining Solution Stock (100×) 100 times with PBS), followed by observation under a fluorescence microscope. Living cells should stain fluorescing green (Ex495/ Em518), while dead cells should appear red (Ex493/ Em620). Then cells were counted by Image-pro plus 5.0 to calculate the live to dead ratio.

2.4.4 Osteogenic gene expression

The osteogenic gene expressions of BMSCs were evaluated using the realtime polymerase chain reaction (Real-time PCR). After 7 days and 14 days of incubation in osteogenic media, the total RNA was isolated using the Trizol reagent and then 1 μg RNA from each sample was reverse transcribed into complementary DNA (cDNA) using the PrimeScript RT reagent kit (TaKaRa). The forward and reverse primers for the selected genes were listed in Table 1 [15, 19]. Expressions of osteogenesis-related genes including runt-related transcription factor 2 (RUNX2), bone morphogenetic protein-2 (BMP-2), bone sialoprotein (BSP), and osteopontin (OPN) were quantified using Real-time PCR (Bio-Rad iQ 5 Multicolor Real-Time PCR Detection System, ABI 7300 USA) with SYBR Premix Ex Taq II (TaKaRa). Data analysis was carried out using the

iQ 5 Optical System Software Version 2.0 (Bio-Rad). The relative expression levels for each gene of interest were normalized to that of the housekeeping gene β-actin.

2.4.5 Statistical analysis

Date was statistically analyzed by means of SPSS11.5 statistical software (Chicago, USA). Comparison and analysis were carried out among the groups using Student–Newman–Keuls post hoc test of one way variance (ANOVA). $P < 0.05$ was considered statistically significant.

3 Results

3.1 Characterization of RGDC-TiO$_2$ nanotubes

3.1.1 SEM

The microstructures of samples were assessed by SEM (Fig. 1). The diameter of the nanotube layers fabricated at 15 V was approximately 70 nm (Fig. 1a). The TiO$_2$ nanotube layers were not changed in APTES after stirring for 2 h (Fig. 1b). There was no clogging after the nanotubes were modified by 1 mM RGDC or 10 mM RGDC (Fig. 1c, d).

3.1.2 XPS analysis

The XPS technique was used to determine the elemental composition of the sample surface. After each step of APTES modification, survey scans were carried out to determine the surface elemental compositions for the various TiO$_2$ nanotubes (Table 2; Fig. 2). The analysis on APTES-modified surfaces revealed that 0.85% of the element on the surface was silicon, suggesting effective APTES binding. The RGDC peptide used in this study includes a sulfur-containing cysteine residue that serves as a marker for the presence of the peptide, so only sulfur was presented in the grafted peptide. After RGDC coupling, the concentrations of carbon and nitrogen increased because of the high proportion of these elements in the RGDC molecules. Our experiment demonstrated there was the sulfur

Table 2 Surface elemental composition of various TiO$_2$ Nanotube layers

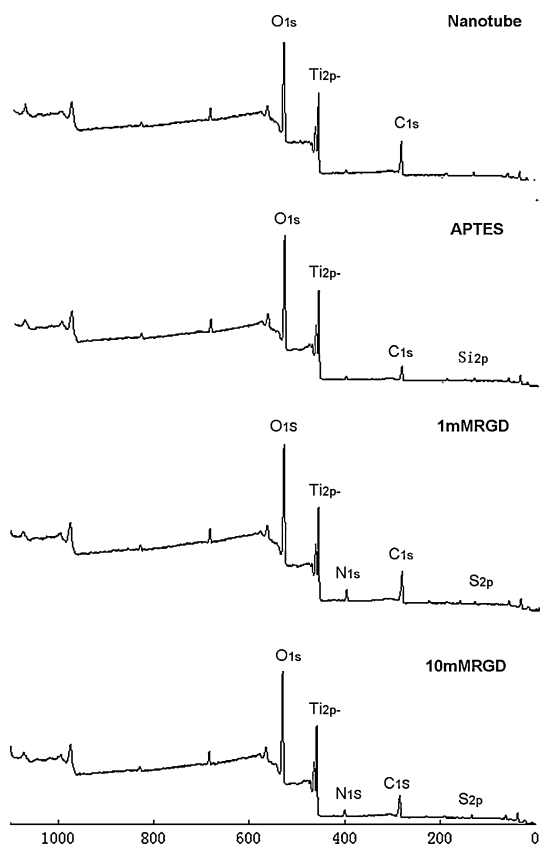|	P(%)	C(%)	N(%)	Ti(%)	O(%)	F(%)	Si(%)	S(%)
(a) Nanotubes	1.64	34.83	2.05	15.74	42.74	3.00	–	–
(b) APTES	1.52	17.59	2.03	20.79	52.89	4.33	0.85	–
(c) RGDC(1 mM)	1.63	26.01	3.88	18.35	46.33	3.40	–	0.40
(d) RGDC(10 mM)	1.30	29.78	5.29	16.11	43.60	2.99	–	0.92

Fig. 2 XPS survey scans for various TiO$_2$ nanotube layers

Table 3 Relative Abundance of Functional Groups as Proportion of Carbon Determined by Peak Fitting of C1s Spectra

	Nanotubes	APTES	1 mM RGD	10 mM RGD
C–C	67.32%	58.06%	56.97%	65.61%
C–O	22.34%	36.81%	29.54%	21.30%
C=O, N–C=O	–	–	7.47%	7.02%
O=C–O	–	–	6.02%	6.07%

element in the RGDC-TiO$_2$ nanotubes sample, indicating successful graft of RGDC peptide on the TiO$_2$ nanotubes surface (Fig. 2).

Peak fitting of the C1s core level revealed the nature of the carbon species for each surface (Table 3; Fig. 3). Nanotubes had the environment with highest proportion of C–C bond (67.32%), which links the fluorenyl group to the peptide. However, a relatively low proportion of C–O (22.34%) and no amide (N–C=O) or carboxyl (O–C=O) was found in the environment.

After silanization and RGDC coupling, the amount of hydrocarbons increased with the exception of carbamate. RGDC-TiO$_2$ Nanotube (1 mM RGD) samples had an intermediate amount of C=O or N–C=O (7.47%), and a low observed proportion of O–C=O (6.02%), showing the
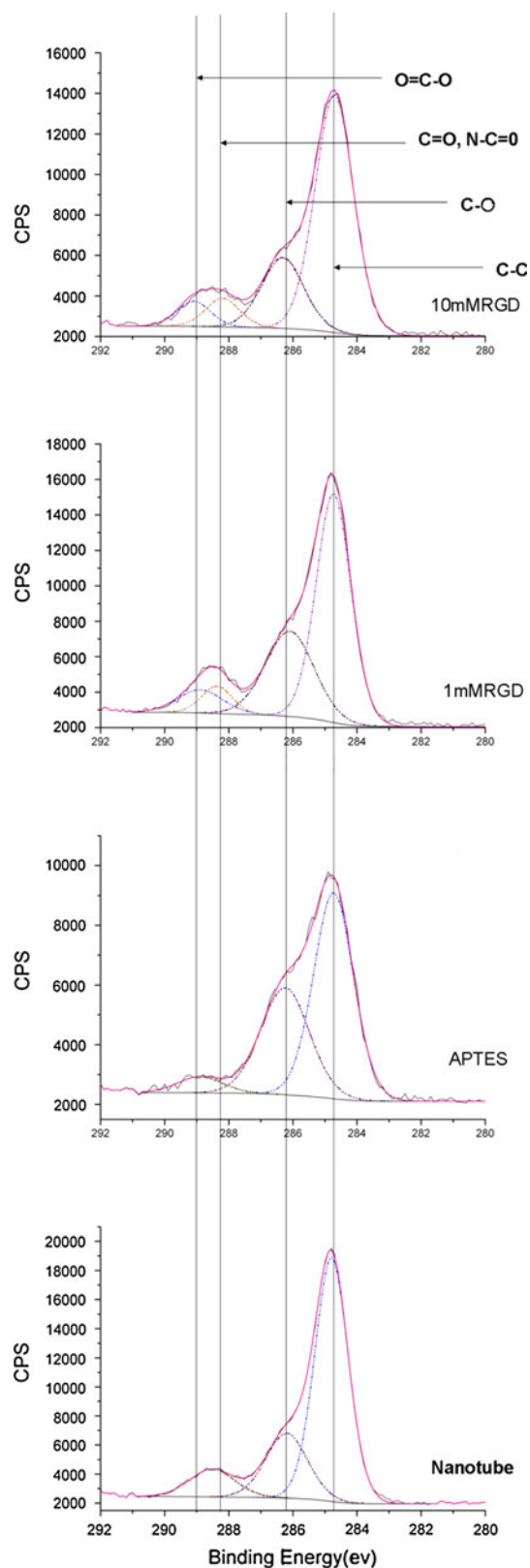

Fig. 3 XPS high-resolution C1s spectrum collected for grafted layers on titanium disks: relative peak positions and intensities of ether (286.3 eV), amide (288.3 eV), and carboxyl (289.0 eV) species have been normalized with respect to the hydrocarbon peak (284.8 eV)
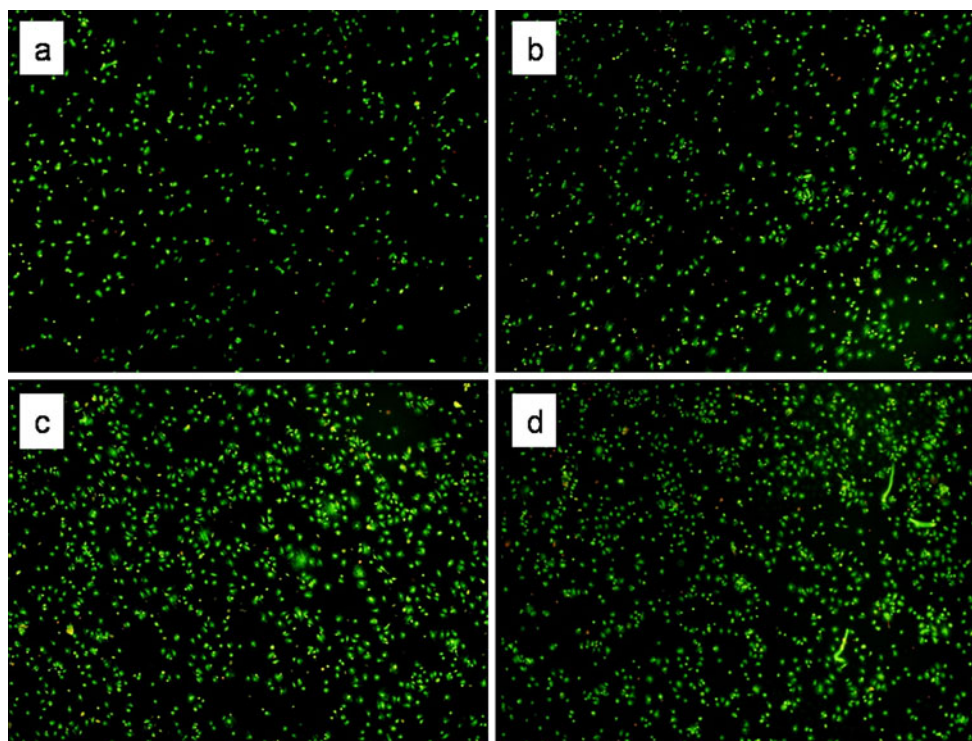
Fig. 4 Visualization of BMSCs on titanium dishes by Live/Dead staining (×40). **a** untreated TiO$_2$ nanotube layers. **b** APTES-silanized TiO$_2$ nanotube layers. **c** 1 mM RGDC-TiO$_2$ nanotube layers. **d** 10 mM RGDC-TiO$_2$ nanotube layers

successful coupling of RGDC. In addition, RGDC-TiO$_2$ Nanotube (10 mM RGD) samples had the similar amount of C=O or N–C=O (7.02%) and O–C=O (6.07%).

3.2 Biological activity

3.2.1 Cell adhesion

Cell adhesion on the specimens was detected after 4 h of incubation. The adherent cell numbers on the silanized and grafted RGDC surfaces were dramatically higher than that on the TiO$_2$ nanotube surface at each time points (Fig. 4). Then cell number on the RGDC-TiO$_2$ nanotube surface was higher than that on the APTES-silanized surfaces ($P < 0.05$). Furthermore, the live to dead ratio on 1 or 10 mM RGDC-TiO$_2$ nanotubes showed similar tendency (Fig. 5).

3.2.2 Cell morphology

The morphology of rat BMSCs on different TiO$_2$ nanotube layers was investigated using SEM technique. High SEM images of cells after 4 h of culture on different TiO$_2$ nanotube layers were revealed, with similar appearance on
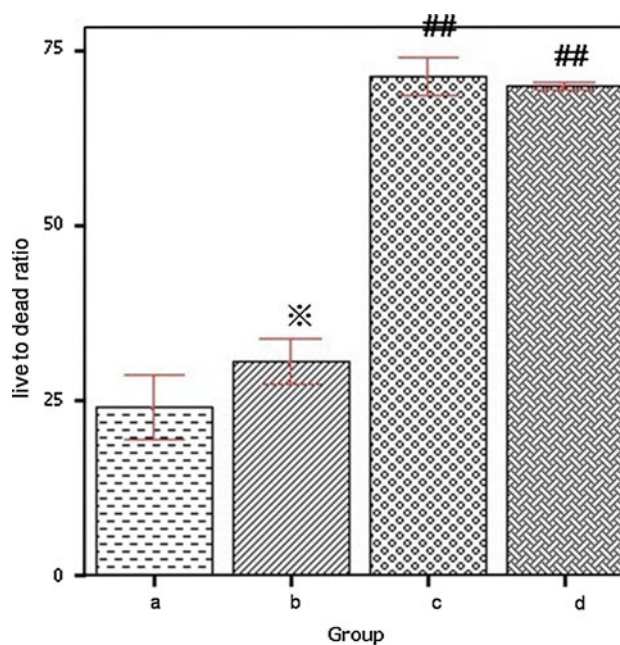

Fig. 5 Count cells and calculate the live to dead ratio. *a* untreated TiO$_2$ nanotube layers. *b* APTES-silanized TiO$_2$ nanotube layers. *c* 1 mM RGDC-TiO$_2$ nanotube layers. *d* 10 mM RGDC-TiO$_2$ Nanotube layers $P < 0.05$ compared with untreated TiO2 nanotube surface
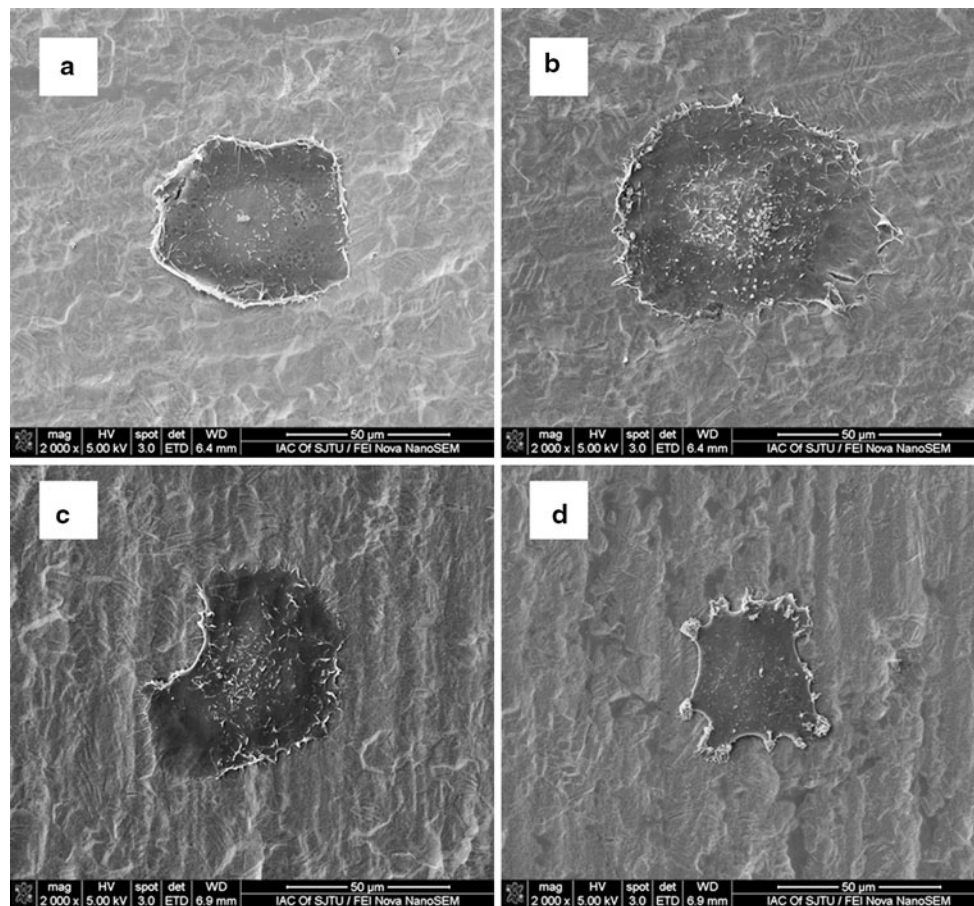
Fig. 6 High magnification SEM images of BMSCs cultured after 4 h on different surfaces. **a** untreated TiO_2 nanotube layers. **b** APTES-silanized TiO_2 nanotube layers. **c** 1 mM RGDC-TiO_2 nanotube layers. **d** 10 mM RGDC-TiO_2 nanotube layers

all the substrates (Fig. 6). After 24 h, BMSCs cultured on the TiO_2 nanotube layers and APTES-silanized surfaces demonstraed the smaller circular or elliptic morphology (Fig. 7a, b). However, the BMSCs cultured on the RGDC-TiO_2 nanotube layers exhibited polygonal morphology and more filopodia (Fig. 7c, d).

3.2.3 Osteogenic-related gene expressions

The gene expressions on the Ti surfaces were quantified using Real-time PCR (Fig. 8). After 1 week of incubation, the 10 mM RGDC-TiO_2 nanotube group showed the highest expression among all the samples for the mRNA of BMP-2, RUNX2, BSP, and OPN. No difference was found in the relative expression levels of these genes among untreated TiO_2 nanotube layers, APTES-silanized TiO_2 nanotube layers, and 1 mM RGDC-TiO_2 nanotube layers ($P > 0.05$). After 2 weeks, the 10 mM RGDC-TiO_2 nanotube surface also exhibited the highest expression levels. Furthermore, the 1 mM RGDC-TiO_2 nanotube surface yields higher expressions for BSP and BMP-2 genes than the TiO_2 nanotube layers ($P < 0.05$). No

different expressions of the genes RUNX2 and OPN were found among TiO_2 nanotube layers surface, APTES-silanized surface, and 1 mM RGDC-TiO_2 nanotube surface ($P > 0.05$).

4 Discussion

To improve biocompatibility, wound healing and the osseointegration around implants, the nanotechnology and peptide immobilization technique are two main methods in modifying Ti implant surfaces. In this study, we immobilized RGD peptide on the TiO_2 nanotubes to modify the Ti implant, resulting in enhanced adhesion and osteogenic gene expression of BMSCs on nanotubes with RGD compared with the nanotubes.

The density of RGDC on titanium plays an important role in cellular behavior [11, 20]. Cell attachment could show an S-type curve as a result of increased RGD concentration [21, 22]. This indicates that there is a critical minimum RGD density for cell response. However, this threshold may be different depending on different material
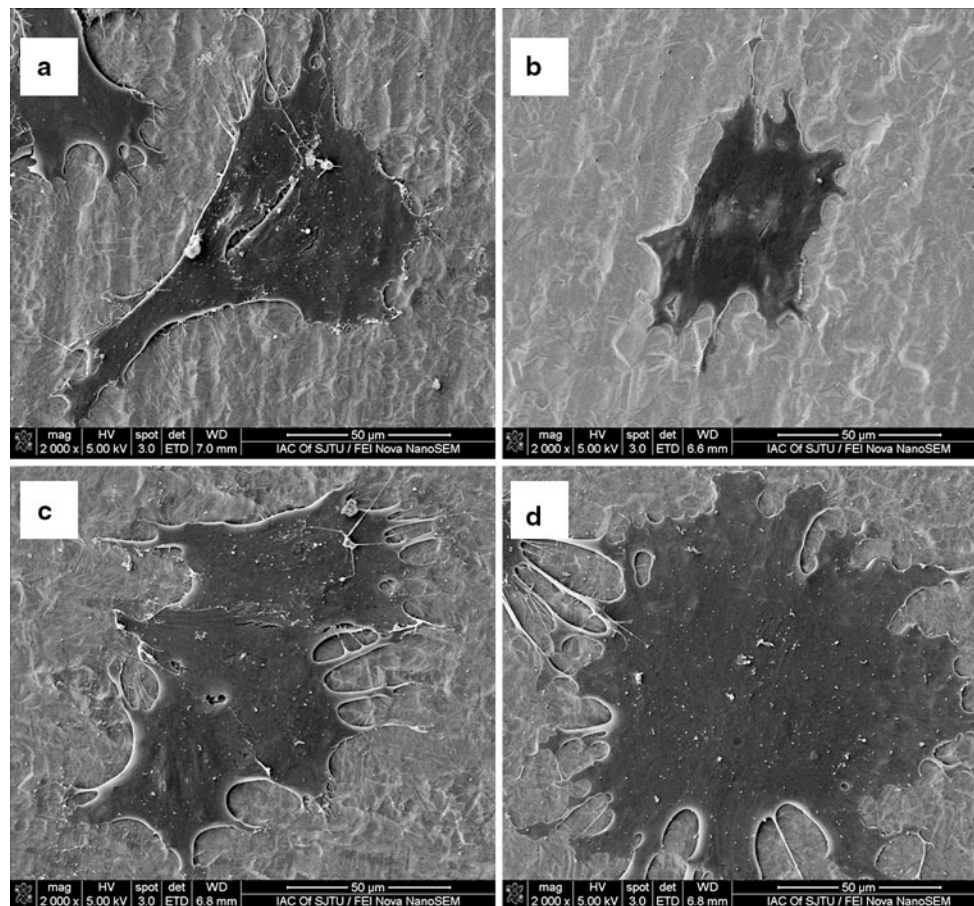
Fig. 7 High magnification SEM images of BMSCs cultured after 24 h on different surfaces. **a** untreated TiO$_2$ nanotube layers. **b** APTES-silanized TiO$_2$ nanotube layers. **c** 1 mM RGDC-TiO$_2$ nanotube layers. **d** 10 mM RGDC-TiO$_2$ nanotube layers

surfaces and cell lines [20]. Kantlehner et al. [21] found that the titanium penetrated in the RGD solution (100 μmol/l) significantly promoted MC3T3 mouse osteoblasts adhesion on the surface. Study showed that 10 mM RGDC modified nanoporous alumina could enhance human fetal osteoblasts (designated hFOB 1.19) adhesion after 1 day of culture and visible matrix production was found after 2 days compared to other groups [17]. Therefore, two different concentrations (high concentrations (10 mM) and low concentrations (1 mM)) of RGDC were adopted in our study to modify TiO$_2$ nanotubes. As an indicator for successful RGDC coupling, sulfur content in 10 mM RGDC-TiO$_2$ nanotube layers was higher than that in 1 mM RGDC-TiO$_2$ nanotube layers in the results of XPS.

The Live/Dead viability assay indicated that the highest survival rate was found in the RGDC modified surface group during the incubation time (Figs. 4, 5). Furthermore, SEM demonstrated that more filopodia was found on the RGDC modified surface after 24 h culture (Fig. 7). The possible explanation for increased BMSCs adhesion on the RGDC modified surface could be that the attachment of peptides promotes living cell survival. This is based upon

the ability of peptides to bind more than one cell adhesion receptor, and their biological impact on cell anchoring, survival and other behaviors [20]. The adhesion process mediated by integrin includes a cascade of four partly overlapping events [23]: cell attachment, cell spreading, organization of actin cytoskeleton, and formation of focal adhesions. During the four steps of cell adhesion, integrins are employed in physical anchoring processes as well as in signal transduction through the cell membrane [24]. About half of the 24 integrins have been shown to bind to ECM molecules in a RGD dependent manner: α3β1, α5β1, α8β1, αIIbβ3, αvβ1, αvβ3, αvβ5, αvβ6, αvβ8, α2β1 and α4β1 [25]. Therefore, the RGD sequence could be called the "universal cell recognition motif". On the other hand, the same adhesion effect found in 1 mM and 10 mM RGDC-TiO$_2$ nanotube layers may be due to saturation of cell surface receptor [20]. Interestingly, results of our studies also showed that amine modified anodized substrates significantly enhanced BMSCs adhesion compared to untreated TiO$_2$ nanotube layers. It may be due to chemical changes of free amino groups resulting from APTES functionalization created regions of highly positively
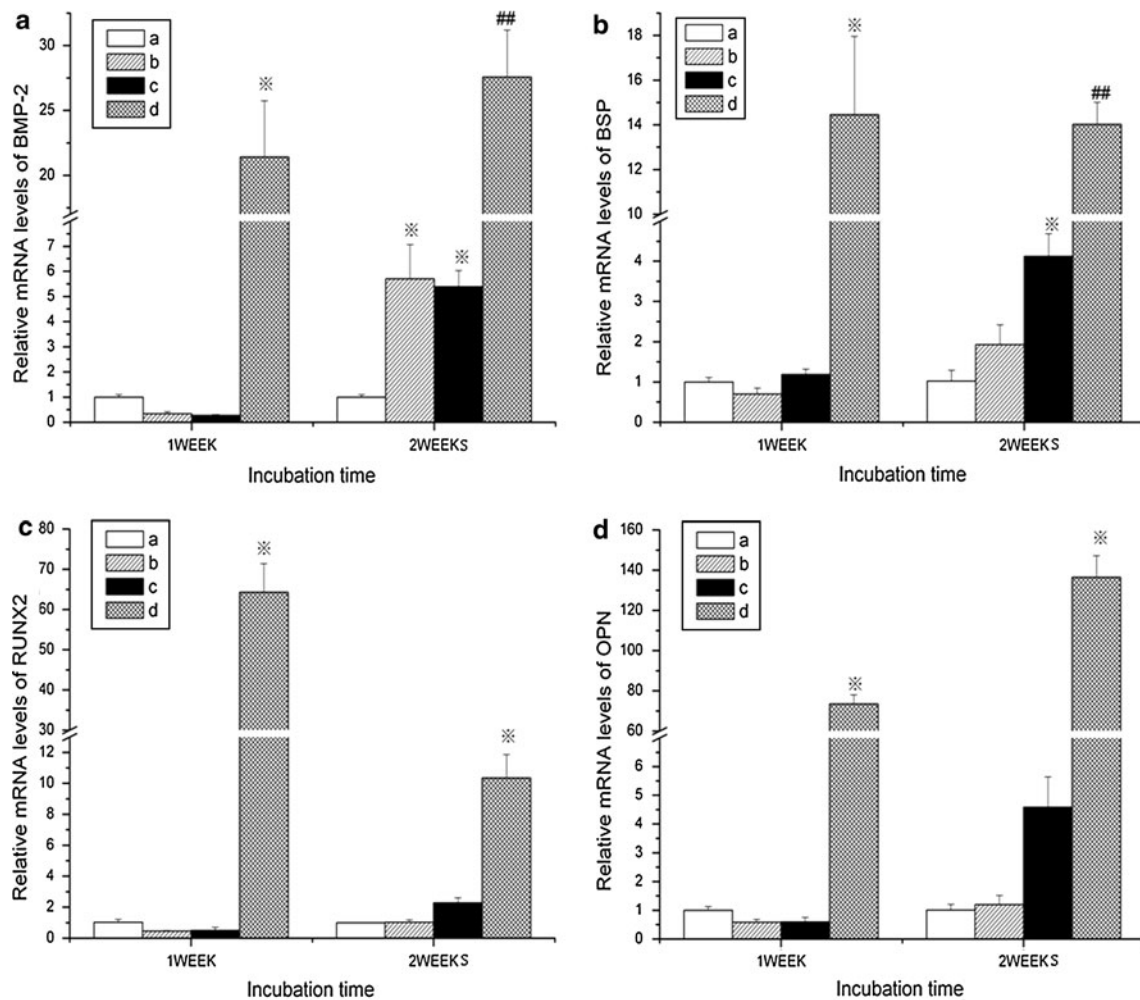
Fig. 8 Gene expressions of BMSCs cultured on titanium surfaces after incubation of 2 weeks. *a* untreated TiO_2 nanotube layers. *b* APTES-silanized TiO_2 nanotube layers. *c* 1 mM RGDC-TiO_2 nanotube layers. *d* 10 mM RGDC-TiO_2 nanotube layers $P < 0.05$ compared with untreated TiO_2 nanotube surface. (**a** Relative m RNA levels of BMP-2. **b** Relative m RNA levels of BSP. **c** Relative m RNA levels of RUNX2. **d** Relative m RNA levels of OPN)

charged densities on Ti [18]. Other studies could also explain our observed phenomenon, which showed that cells are easy to adhere to cationic surfaces in a charge-dependent manner [26–28].

RGD peptides not only act as anchoring molecules but also play an important role in processes of cell differentiation [20]. In this study, 10 mM RGDC-TiO_2 nanotube layers could significantly increase mRNA expression of osteogenesis-related genes including BMP-2, RUNX2, BSP, and OPN. This could be explained by astrocytic adhesion and migration mediated by binding of RGD to integrin $\alpha v \beta 3$ or $\alpha 5 \beta 1$ [20], or explained by direct effects on integrins in migration process by some features of RGD functionalized surfaces. In addition, the RGD is supposed to play an important role in the control of bone cell differentiation [15]. In particular, $\alpha v \beta 3$ and $\alpha v \beta 5$ integrin-selective RGD peptide ligands were responsible for

adjusting the initial adhesion and subsequent synthesis of mineralized matrix [29]. Wang et al. [30] and Ruoslahti [31] have reported that the interaction of the RGD-ligand and integrin receptors was characterized by an increased level of gene transcription and the triggering of cytodifferentiation pathway. In our study, 1 mM RGDC-TiO_2 nanotube layers only slightly promoted cell differentiation compared with 10 mM RGDC-TiO_2 nanotubes. Cell interactions with RGD – containing peptide epitopes could be affected not only by the conformation and chemical properties of matrix-derived peptide epitopes, but also by their spatial distribution and density [15]. The 10 mM RGDC-TiO_2 nanotubes might provide more suitable spatial distribution and density for cell differentiation, which may explain enhanced differentiation by 10 mM RGDC-TiO_2 than 1 mM RGDC-TiO_2 nanotubes. Further experiments were needed to confirm this hypothesis.

5 Conclusion

In this study, the cell adhesion peptide RGD was immobilized covalently on the TiO$_2$ nanotube layer, which was characterized by XPS technique. Our results demonstrated that TiO$_2$ nanotube layers modified with RGD were convenient for BMSCs adhesion and osteogenic gene expression compared with the TiO$_2$ nanotube layers. This study suggests that the nanotubular Ti modified with adhesion peptide may be used as dental or orthopedic implants. Further studies will be needed to test the bone regeneration in vivo.

References

1. Linder L, Carlsson A, Marsal L, Bjursten LM, Brånemark PI. Clinical aspects of osseointegration in joint replacement. A histological study of titanium implants. J Bone Joint Surg Br. 1988; 70:550–5.
2. Avila G, Misch K, Galindo-Moreno P, Wang HL. Implant surface treatment using biomimetic agents. Implant Dent. 2009;18: 17–26.
3. Nishimoto SK, Nishimoto M, Park SW, Lee KM, Kim HS, Koh JT, Ong JL, Liu Y, Yang Y. The effect of titanium surface roughening on protein absorption, cell attachment, and cell spreading. Int J Oral Maxillofac Implant. 2008;23:675–80.
4. Mendonça G, Mendonça DB, Aragão FJ, Cooper LF. Advancing dental implant surface technology: from micron - to nanotopography. Biomaterials. 2008;29:3822–35.
5. Oh S, Daraio C, Chen LH, Pisanic TR, Finones RR, Jin S. Significantly accelerated osteoblast cell growth on aligned TiO$_2$ nanotubes. J Biomed Mater Res A. 2006;78:97–103.
6. Bjursten LM, Rasmusson L, Oh S, Smith GC, Brammer KS, Jin S. Titanium dioxide nanotubes enhance bone bonding in vivo. J Biomed Mater Res A. 2010;92:1218–24.
7. Oh S, Brammer KS, Li YS, Teng D, Enqler AJ, Chien S, Jin S. Stem cell fate dictated solely by altered nanotube dimension. Proc Natl Acad Sci USA. 2009;106:2130–5.
8. Yu WQ, Jiang XQ, Zhang FQ, Xu L. The effect of anatase TiO2 nanotube layers on MC3T3–E1 preosteoblast adhesion, proliferation, and differentiation. J Biomed Mater Res Part A. 2010;94: 1012–22.
9. Ruoslahti E, Pierschbacher MD. Arg-Gly-Asp: a versatile cell recognition signal. Cell. 1986;44:517–8.
10. Porté-Durrieu MC, Labrugère C, Villars F, Lefebvre F, Dutoya S, Guette A. Development of RGD peptides grafted onto silica surfaces: XPS characterization and human endothelial cell interactions. J Biomed Mater Res. 1999;46:368–75.
11. Arnold Marco, Ada Cavalcanti-Adam Elisabetta, Glass Roman. Activation of Integrin Function by nanopatterned adhesive Interfaces. Chem Phys Chem. 2004;5:383–8.
12. Xiao SJ, Textor M, Spencer ND, Wieland M, Keller B, Sigrist H. Immobilization of the cell-adhesive peptide Arg-Gly-Asp-Cys (RGDC) on titanium surfaces by covalent chemical attachment. J Mater Sci Mater Med. 1997;8:867–72.
13. Wang D, Ji J, Sun Y, Shen JC, Feng LX, Elisseeff JH. In situ immobilization of proteins and RGD peptide on polyurethane surfaces via poly(ethylene oxide) coupling polymers for human endothelial cell growth. Biomacromolecules. 2002;3:1286–95.
14. Schliephake H, Scharnweber D, Dard M, Rossler S, Sewing A, Meyer J, Hoogestraat D. Effect of RGD peptide coating of titanium implants on peri-implant bone formation in the alveolar crest. An experimental pilot study in dogs. Clin Oral Implant Res. 2002;13:312–9.
15. Secchi AG, Grigoriou V, Shapiro IM. RGDS peptides immobilized on titanium alloy stimulate bone cell attachment, differentiation and confer resistance to apoptosis. J Biomed Mater Res A. 2007;83:577–84.
16. Kim HS, Yang Y, Koh JT, Lee KK, Lee KM, Park SW. Fabrication and characterization of functionally graded nano-micro porous titanium surface by anodizing. J Biomed Mater Res B Appl Biomater. 2009;88:427–35.
17. Swan EE, Popat KC, Desai TA. Peptide-immobilized nanoporous alumina membranes for enhanced osteoblast adhesion. Biomaterials. 2005;26:1969–76.
18. Balasundaram Ganesan, Yao Chang, Thomas J. Webster. TiO$_2$ nanotubes functionalized with regions of bone morphogenetic protein-2 increases osteoblast adhesion. J Biomed Mater Res Part A. 2008;84:447–53.
19. De Giglio E, Cometa S, Calvano CD, Sabbatini L, Zambonin PG, Colucci S, Benedetto AD, Colaianni G. A new titanium biofunctionalized interface based on poly(pyrrole-3-acetic acid) coating: proliferation of osteoblast-like cells and future perspectives. J Mater Sci Mater Med. 2007;18:1781–9.
20. Hersel U, Dahmen C, Kessler H. RGD modified polymers: biomaterials for stimulated cell adhesion and beyond. Biomaterials. 2003;24:4385–415.
21. Kantlehner M, Schaffner P, Finsinger D, Meyer J, Jonczyk A, Diefenbach B, Nies B, Holzemann G, Goodman SL. Surface coating with cyclic RGD peptides stimulates osteoblast adhesion and proliferation as well as bone formation. Chem BioChem. 2000;1:107–14.
22. Jeschke B, Meyer J, Jonczyk A, Kessler H, Adamietz P, Meenen NM, Kantlehner M, Goepfert C, Nies B. RGD-peptides for tissue engineering of articular cartilage. Biomaterials. 2002;23:3455–63.
23. Lebaron RG, Athanasiou KA. Extracellular matrix cell adhesion peptides: functional applications in orthopedic materials. Tissue Eng. 2000;6:85–103.
24. van der Flier A, Sonnenberg A. Function and interactions of integrins. Cell Tissue Res. 2001;305:285–98.
25. Takagi J. Structural basis for ligand recognition by RGD (Arg-Gly-Asp)-dependent integrins. Biochem Soc Trans. 2004; 32:403–6.
26. Massia SP, Hubbell JA. Covalent surface immobilization of Arg-Gly-Asp- and Tyr-Ile-Gly-Ser-Arg-containing peptides to obtain well-defined cell-adhesive substrates. Anal Biochem. 1990;187:292–301.
27. Anselme K. Osteoblast adhesion on biomaterials. Biomaterials. 2000;21:667–81.
28. Nelson M, Balasundaram G, Webster TJ. Increased osteoblast adhesion on Ti functionalized with KRSR. J Biomed Mater Res A. 2007;80:602–11.
29. Pallu S, Bareille R, Dard M, Kessler H, Jonczyk A, Vernizeau M, Amédée-Vilamitjana J. A cyclo peptide activates signaling events and promotes growth and the production of the bone matrix. Peptides. 2003;24:1349–57.
30. Wang N, Butler JP, Ingber E. Mechanotransduction across the cell surface and through the cytoskeleton. Science. 1993;260: 1124–7.
31. Ruoslahti E. RGD and other recognition sequences for integrins. Annu Rev Cell Dev Biol. 1996;12:697–715.